Parasite infection induces size-dependent host dispersal: consequences for parasite persistence

Akira Terui[1, 2]*, Keita Ooue[2], Hirokazu Urabe[3], Futoshi Nakamura[2]

Affiliation:

[1]Department of Ecology, Evolution, and Behavior, University of Minnesota, 1479 Gortner Avenue, St. Paul, MN 55108, USA

[2]Department of Forest Science, Graduate School of Agriculture, Hokkaido University, Kita 9, Nishi 9, Kita-ku, Sapporo 060-8589, Japan

[3]Salmon and Freshwater Fisheries Research Institute, Hokkaido Research Organization, 3-373 Kitakashiwagi, Eniwa, 061-1433, Japan,

* Corresponding author

Tel., Fax: +81 11 706 3842

E-mail address: hanabi0111@gmail.com (A. Terui)

Abstract

Host dispersal is now recognized as a key predictor of the landscape-level persistence and expansion of parasites. However, current theories treat post-infection dispersal propensities as a fixed trait, and the plastic nature of host's responses to parasite infection has long been underappreciated. Here, we present a mark-recapture experiment in a single-host parasite system (larval parasites of the freshwater mussel *Margaritifera laevis* and its salmonid fish host *Oncorhynchus masou masou*) and provide the first empirical evidence that parasite infection induces size-dependent host dispersal in the field. In response to parasite infection, large fish become more dispersive, whereas small fish tend to stay at the home patch. The observed plasticity in dispersal is interpretable from the viewpoint of host fitness: expected benefits (release from further infection) may exceed dispersal-associated costs for individuals with high dispersal ability (i.e., large fish) but are marginal for individuals with limited dispersal ability (i.e., small fish). Indeed, our growth analysis revealed that only small fish hosts incurred dispersal costs (reduced growth). Strikingly, our simulation study revealed that this plastic dispersal response of infected hosts substantially enhanced parasite persistence and occupancy in a spatially structured system. These results suggest that dispersal plasticity in host species is critical for understanding how parasites emerge,

spatially spread, and persist in nature. Our findings provide a novel starting point for building a reliable, predictive model for parasite/disease management.

Key words: dispersal, plasticity, Bayesian statistics, freshwater mussel, salmon

Introduction

The rising tide of infectious parasites has motivated parasite/disease ecologists to establish the factors that influence parasite persistence and expansion in nature [1-3]. Classic studies have explored basic rules for parasite persistence in a locally well-mixed host population and advance the concept of “critical community size” (i.e., the threshold host density below which a parasite species cannot persist) [3]. More recently, however, researchers have begun to recognize the importance of large-scale spatial processes, in which host dispersal plays a pivotal role in mediating spatial expansion of locally infected host groups/parasite-contaminated habitats [4-6]. In general, parasites *per se* have a very limited dispersal capability [7]. Hence, host dispersal is a primary determinant for the landscape-level dynamics of spatially structured parasite populations [5-7].

Host dispersal is thought to be an effective behavior that enables host individuals to escape from parasite-contaminated habitats [8-10]. However, the evolutionarily stable strategy [11] of infected host’s dispersal depends on the cost-benefit balance of dispersal: if dispersal ensures the avoidance of further infection risks with little or no mortality, theory predicts that natural selection favors increased dispersal tendencies of infected hosts (and *vice versa*) [10]. Predicting such parasite-

induced changes in host dispersal behavior is a crucial issue of parasite/disease ecology, since host dispersal propensity drives the spatial spread of parasites in the landscape [5, 6]. However, current theories build on the implicit assumption that dispersal changes in response to parasite infection are constant within a single host species (i.e., a fixed trait) [10]. Host populations are heterogeneous entities of individuals with varying phenotype (e.g., body size), and the net benefits of dispersal may depend on pre-infection individual status. For example, the inherent costs of dispersal, such as reduced energy reserves or survival [12], may outweigh its potential benefits if the host's performance is insufficient to survive consecutive dispersal processes (i.e., departure, transition, and settlement [13]). Hence, individual-level variation likely exists among post-infection dispersal propensities (i.e., a plastic response). Nevertheless, neither theoretical nor empirical studies have explored the possibility of plastic post-infection dispersal (conditional on individual phenotype) to date, and its potential consequences for spatially structured parasite populations are virtually unknown.

Here, we investigate whether a host species shows plastic post-infection dispersal propensities by using a tractable host-parasite system: larval parasites of the Japanese freshwater mussel *Margaritifera laevis* and its salmonid host *Oncorhynchus masou masou*. As with many metazoan parasites, the life cycle of *M. laevis* can be

76 divided into free-living and obligate parasitic stages [cf. 7]. The free-living animals of
77 *M. laevis* are sedentary, stream-dwelling benthic organisms (mussels) broadcasting
78 millions of larval parasites (glochidia): their larvae are obligate, external parasites on
79 the gills of masu salmon *O. m. masou* (or subspecies *O. m. ishikawae*) [14]. After a 40–
80 50-day parasitic period, glochidia transform into juvenile mussels [14], which recruit
81 into existing mussel aggregations or invade into unoccupied, parasite-free habitats via
82 host dispersal (Fig. 1; [15, 16]). Thus, host dispersal is a key factor determining the
83 landscape-level expansion of the parasite species [15, 16].
84 This single-host parasite interaction (no intermediate host or direct host-to-host
85 transmission) serves as an excellent model system to test how host individuals respond
86 to parasite infection, for the following reasons. First, salmonid populations have a clear
87 size structure with a competitive dominance hierarchy [17, 18], and their body size is
88 known to vary positively with total energy reserves (e.g., time until fatigue) and
89 swimming ability [19]. Therefore, salmonid body size may be a simple, but powerful
90 predictor of post-infection dispersal propensities. Second, Margaritiferidae employ a
91 simple infection strategy by which drifting glochidia released from female mussels
92 parasitize the gills of salmonid hosts [14, 20]. The infection status of masu salmon
93 (infected or uninfected) can be readily manipulated, allowing us to experimentally

compare the dispersal propensity between infected and uninfected fish hosts in the field. Finally, these host and parasite species inhabit relatively small streams, where direct observation of host dispersal is highly feasible [21].

In this study, we tested the hypothesis that glochidial infection induces size-dependent dispersal in salmonid fish hosts. Specifically, we predicted that glochidial infection enhances the dispersal tendency of large fish hosts, while suppressing that of small fish. We directly compared dispersal kernels between uninfected and infected fish using data from 215 marked individuals, half of which were artificially infected with *M. laevis* glochidia. We also examined how host fitness (growth rate) varied with dispersal distance and tested the hypothesis that small fish host have higher costs of dispersal than large fish. Finally, to predict the consequences of the observed host dispersal on landscape-level persistence and expansion of the parasite, we carried out a simulation study in a one-dimensional landscape of 100 habitat patches.

Methods

Study site and study species

We conducted this study in the Chitose river system, Hokkaido, Japan. In Hokkaido,

glochidia of *M. laevis* (~50 μm in shell length [14]) are released in the summer, from mid- to late-July [15, 22], and infect the gills of masu salmon (Fig. 1). Female mussels release synchronously millions of glochidial parasites into the water column (~4 million glochidia per female; [14, 15]), causing extremely high prevalence of glochidial infection near dense mussel aggregations (~100% for hundreds of fish hosts) [15, 16]. The proportion of infected fish declines sharply with distance from the infection source [15]. The maximum life span of *M. laevis* is ~79 years [14]. *Margaritifera laevis* is the only species of freshwater mussel within the river system.

Adult masu salmon spawn in the autumn, and eggs hatch and develop into juvenile salmon (parr) by early summer. The population of available hosts during the brooding period of *M. laevis* (beginning in July) is composed mainly of parr (fish at age 0+), which are suitable hosts for Margaritiferidae [23, 24].

We conducted a mark-recapture experiment in the Osatsu stream (42°50'N 141°36'E), a small tributary flowing into the Chitose river. This spring-fed stream serves as a suitable experimental venue because 1) this system is characterized by little temporal variation in water temperature (range: 4–12 °C) and discharge [25], and because 2) *M. laevis* does not occur in this stream (confounding *M. laevis* infection can be avoided). Field surveys were approved by the Hokkaido prefecture, and all research

was performed in line with the Animal Care and Use guideline of Hokkaido University.

Mark-recapture experiment

We selected a 1,200-m stretch of the Osatsu stream with a 3.0–6.0-m wetted width, where local habitat conditions varied little along the stream stretch, and no apparent dispersal barriers existed. The stretch was divided into 60 capture subsections (each 20 m in length). The first capture session was carried out from July 21 to 24, 2015, and the recapture session occurred ca. 50 days later (Sep 8–11, 2015). This capture-recapture interval was intended to mimic the duration of glochidial infection under the summer water temperature of the Osatsu stream (~12 °C) [26].

During the first capture session, we collected host fish using consecutive three-pass electrofishing in each subsection [27]. We anesthetized captured fish in a 2-phenoxyethanol solution and measured their fork length (millimeters) and wet mass (0.1 g). We batch-marked them with fluorescent visible implant elastomer tags (Northwest Marine Technologies, Shaw Island, Washington) applied to three adipose locations (behind the eye, behind the nose, and the lower jaw). We used six tag colors, and the combination of tag color and position allowed the identification of individual fish (6^3 = 216 patterns). We allowed marked fish to recover in a container for 10–15 min. We did

not mark 1+ fish hosts as they have been identified as unsuitable hosts for Margaritiferids [23, 24].

Half the marked fish collected from each individual subsection were infected with *M. laevis* glochidia by placing them into an infection bath (5-L bucket, 4×10^4 glochidia L^{-1}) for 30 minutes. The other half was kept in a "sham" infection bath with no glochidia (control). This experimental design isolates infection-treatment effects from any environmental variation among subsections. We obtained a preliminary confirmation that this glochidial density provides no infection failure and natural levels of glochidial load (48 ± 29 glochidia per fish), based on the level commonly observed in the Chitose river [22, 28]. We created the infection bath using fresh viable glochidia that were naturally released from a total of four gravid *M. laevis* females (collected every morning from a single population of the Chitose river). The averages and variance of fish body size (fork length) were almost identical between infected and uninfected fish groups (t-test, $P = 0.18$; mean for uninfected fish = 92.5±11.2 mm, mean for infected fish = 90.5±11.2 mm).

Marked fish were then released near the center of the subsection where they were caught. We completed all procedures from 7:00 to 15:00 in light of the short longevity of glochidia [29]. We marked a total of 215 individuals.

At the recapture session, we recaptured marked fish with three-pass electrofishing in each of the subsections. The longitudinal position (recorded as subsection ID, 1–60), fork length, and wet mass of all recaptured fish were recorded.

Dispersal model coupled with observation process

We employed the Laplace (double exponential) kernel, which has been proven to provide adequate fits to dispersal data in various salmonid fish [30, 31]. The Laplace density function, f_L, has a symmetrical exponential decay to either side of the origin, with the inverse of parameter τ equal to the mean dispersal distance (i.e., smaller values of τ indicate greater dispersal tendency):

$$f_L(x_{j(i)}, \mu_i, \tau_i) = \frac{1}{2}\ \tau_i \exp(-\tau_i\ |x_{j(i)} - \mu_i|) \qquad \text{Eq.1}$$

where $x_{j(i)}$ is the distance class (i.e., distance to the downstream end of the whole study section) at the center of recapture subsection j (subscript $j(i)$ denotes jth subsection in which fish individual i was recaptured), and μ_i is the distance class at the center of the capture subsection for fish individual i. It is important to note that the variance ($2/\tau_i^2$) nonlinearly increases with increasing mean dispersal distance ($1/\tau_i$). Thus, the model

can express outliers adequately (i.e., robust to outlier data), which is typical for dispersal data [30, 32]. We related the mean dispersal distance to individual-level predictors with a log-link function:

$$\log(1/\tau_i) = \beta_0 + \beta_1 \cdot Infection_i + \beta_2 \cdot Size_i + \beta_3 \cdot Infection_i \cdot Size_i \quad \text{Eq. 2}$$

where β_0 is an intercept and β_1–β_3 are standardized regression coefficients of infection status $Infection_i$ (binary variable; infected = 1, uninfected = 0), initial body size $Size_i$ (continuous variable; standardized with a mean 0 and SD 1) and their interaction. As initial body size was standardized, parameter β_0 indicates the average $1/\tau$ of the population in a logarithmic scale. This formulation allows us to evaluate the effects of individual-level predictors on the form of dispersal kernels.

To incorporate sampling designs into the parameter inference of dispersal kernels, we modified the inference framework proposed by Pepino *et al.* [31]. The binary variable of capture history Y_i (Y_i = 1 if recaptured, otherwise 0) was modeled based on a Bernoulli distribution (see Electronic Supplementary Material for derivation),

$$Y_i \sim \text{Bernoulli}(\varphi_{j(i)} s_i D_i) \quad \text{Eq. 3}$$

where $\varphi_{j(i)}$ is the section-specific probability of capture and s_i is the survival probability during the study period. For recaptured individuals, D_i is the probability that individual i moves from release point μ_i to subsection of recapture j. For unrecaptured individuals, D_i represents the probability of staying in the 1,200-m study stretch:

$$D_i = \begin{cases} \int_{x_{j(i),low}}^{x_{j(i),up}} f_L(x_{j(i)}, \mu_i, \tau_i) dx_{j(i)}, & \text{if recaptured} \\ \int_{Low}^{Up} f_L(x_{j(i)}, \mu_i, \tau_i) dx_{j(i)}, & \text{if unrecaptured} \end{cases} \quad \text{Eq. 4}$$

where $x_{j(i),up}$ and $x_{j(i),low}$ are the distance classes at the upper and lower boundaries of the recapture subsection j for individual i, and *Up* and *Low* are the distance classes at the upper (1,200 m) and lower ends (0 m) of the whole study section. Individual-specific survival probability s_i is an identifiable parameter, as we obtained an independent estimate of section-specific capture probability $\varphi_{j(i)}$ using the three-pass depletion surveys with a Bayesian modification (see Electronic Supplementary Material) [27]. Survival probability was normally distributed in a logit scale: $\text{logit}(s_i) \sim \text{Normal}(\text{logit}(s_{global}), \sigma_s^2)$, where s_{global} represents the mean survival probability.

However, it was impossible to determine $\varphi_{j(i)}$ for unrecaptured individuals,

since we have no information on subsection ID of recapture. Instead, for unrecaptured individuals, we estimated the weighted mean of $\varphi_{j(i)}$ across subsections ($\varphi_{w,i}$) given the dispersal parameter τ_i:

$$\varphi_{w,i} = \sum_{j=1}^{60} w_{j(i)} \varphi_j \quad \text{Eq. 5}$$

$$w_{j(i)} = \frac{\int_{x_{j(i),low}}^{x_{j(i),up}} f_L(x_{j(i)}, \mu_i, \tau_i) dx_{j(i)}}{\int_{Low}^{Up} f_L(x_{j(i)}, \mu_i, \tau_i) dx_{j(i)}} \quad \text{Eq. 6}$$

In equation 6, the numerator indicates the probability of movement from release point μ_i to *j*th subsection (i.e., the probability of unrecaptured individual *i* present at *j*th subsection during the recapture session). The denominator (the probability of staying in the 1,200-m study stretch) scales the numerator so that $\sum_{j=1}^{60} w_{j(i)}$ equals 1.0.

Vague priors were assigned to the parameters: normal distributions for β (mean = 0, variance = 10^4), a beta distribution for s_{global} (shape = 1, scale = 1), and a truncated normal distribution for σ_s^2 (mean = 0, variance = 10^4, range = 0–100) The model was fitted to the data with JAGS ver. 4.1.0 and the package ‘‘*runjags*’’ [33] in R 3.3.1 [34]. Three Markov chain Monte Carlo (MCMC) chains were run with 9,000 iterations (3,000 burn-in), and 500 samples per chain were used to calculate posterior probabilities. Convergence was assessed by examining whether the R-hat indicator of

each parameter approached 1 [35].

Host growth analysis

We analyzed factors that influence host growth using data from recaptured fish (n = 116). We estimated individual host growth G as:

$$G = \log(FL_{50}/FL_0) \quad \text{Eq. 7}$$

where FL_0 and FL_{50} denote fork length at capture and recapture, respectively.

We then constructed a linear mixed effect model with a random effect of initial capture subsection ID to investigate factors influencing host growth G. Host growth G was assumed to follow a normal distribution and was modeled as a function of distance moved (continuous), logarithm of fork length at initial capture ($\log(FL_0)$; continuous), infection (binary), and their two-way interactions. Continuous explanatory variables were standardized prior to the analysis (mean = 0, SD = 1). However, an analytical issue can arise when using G as a response variable: $\log(FL_0)$ will appear in both sides of the equation, causing spurious correlations [36]. To avoid this analytical issue, we put $\log(FL_0)$ in the response variable into the right side (i.e., offset term): $\log(FL_{50}) = \mathbf{X\beta} +$

256 $\varepsilon + \log(FL_0)$, where **X** is a matrix of predictors, **β** is a vector of regression coefficients,
257 and ε is the random effect of initial capture subsection ID.
258 Vague priors were assigned to regression coefficients (normal distributions:
259 mean = 0, variance = 1,000) and standard deviations of residuals and the random effect
260 (uniform distributions: range, 0–100). Three MCMC chains were run with 15,000
261 iterations (5,000 burn-in) using JAGS, and 500 samples per chain were used to calculate
262 posterior probabilities. Convergence was assessed as indicated above.
263
264 *Simulation*
265 To investigate the consequences of the observed dispersal probabilities on the
266 landscape-level expansion and persistence of the parasite, we modified a simulation
267 model described by Grant *et al.* [37]. In our simulation, we assumed a linear landscape
268 of 100 habitat patches of equal quality and length (20 m). Simulation space boundaries
269 were wrapped. We initially introduced five parasite-occupied patches into the landscape
270 (5% occupancy), and a random, independent patch-extinction of parasite-occupied patch
271 occurred with the probability *E* in each time step (i.e., transition from a parasite-
272 occupied to parasite-free patch). After random extinction events of parasite-occupied
273 patches, we allowed immediate (re)colonization of mussel aggregation (i.e., transition

from a parasite-free to parasite-occupied patch) from other parasite-occupied patches through host dispersal (Fig. 1): in each time step *t*, all host fish at parasite-occupied patch *i* ($N_{i,t}$) were infected with glochidia (100% prevalence of local glochidial infection; [15, 16]) and dispersed randomly based on the predefined Laplace dispersal kernels (see below). Every host dispersers had information on its own position (i.e., distance [m] to the downstream end). During dispersal, infected host fish survived with the probability *s* (*s* = 0.87; see Results), and each surviving individual that reached a parasite-free patch *j* (i.e., between $x_{j(i),low}$–$x_{j(i),up}$) had the potential to create a new infection source (parasite-occupied patch) with the probability *C*. Thus, the realized per-fish colonization probability is the product of *s* and *C*. Host fish present at parasite-free patches (i.e., no mussel aggregation) were not considered as dispersal agents.

The number of host fish at patch *i* at time step *t* was drawn from a Poisson distribution as $N_{i,t} \sim \text{Poisson}(\lambda_t)$. This reflects real situations: that is, in each time step, newly emerged susceptible hosts (i.e., 0+ fish of the year) were randomly (re)distributed across the simulation space. The mean host density (fish/patch) at time step *t*, λ_t, was determined by the Ricker model [38-40]:

$$\log(\lambda_{t+1}) = r - b \cdot \lambda_t + \log(\lambda_t) + \varepsilon_t \qquad \text{Eq. 8}$$

where r is the intrinsic population growth rate, b is the parameter that determines negative density dependence, and ε_t is the environmental stochasticity. In this formulation, the host carrying capacity K can be written as r/b. The parameter ε_t is governed by a normal distribution with a mean of 0 and variance of σ_ε^2, and the variance parameter σ_ε^2 determines the degree of environmental stochasticity. Host population dynamics were assumed to be independent of parasite infection, as we did not find negative effects of glochidial infection on fish growth (see Table 2).

The dispersal parameter τ_i for the Laplace density function was described as follows:

$$\log(1/\tau_i) = \gamma + \delta \cdot z_i \qquad \text{Eq. 9}$$

where γ is the intercept, δ is the slope that determines the strength of size-dependence in host dispersal, and z_i is the standardized random variable of body size, $z_i \sim \text{Normal}(0, 1)$. Note that the parameters (γ and δ) can be substituted by empirical dispersal estimates in equation 2: $\log(1/\tau_i) = [\beta_0 + \beta_1 \cdot \mathit{Infection}_i] + [\beta_2 + \beta_3 \cdot \mathit{Infection}_i] \cdot \mathit{Size}_i$. This representation allowed us to predict the consequences of observed dispersal patterns on

parasite persistence (control [*Infection* = 0]: $\gamma = \beta_0$, $\delta = \beta_2$; treatment [*Infection* = 1]: $\gamma = \beta_0 + \beta_1$, $\delta = \beta_2 + \beta_3$).

We examined 16 dispersal parameter combinations (γ = 1.5, 2.0, 2.5, 3.0; δ = 0.0, 0.5, 1.0, 1.5) that cover the empirical estimates (see Results). We also set the following parameters: C = 0.005, E = 0.01, K = 4 or 8, r = 1.43, and σ_ε = 0.18. Per-fish colonization rate C was parameterized according to the reported mussel mortality during their early benthic life stage (~99.5%) [41]. Specific estimates of annual per-patch extinction probability were not available, but descriptive evidence suggests that the parameter should be $\leq$ 0.01 [42]. The range of parameter K was determined based on the masu salmon density in the Osatsu stream (0–12 fish per 20-m subsection). We used fixed values of r and σ_ε based on a meta-analysis by Myers *et al.* [39], and the density-dependence parameter b was calculated as r/K. For a connection with traditional epidemiological parameters (e.g., the basic reproductive number R_0), see Electronic Supplementary Material.

We ran the simulation model for a maximum of 10,000 time steps. We obtained persistence time of the spatially structured parasite population (time to the entire extinction of parasite-occupied patch) and median proportion of parasite-occupied patch (hereafter, “occupancy”) during the persistent period (i.e., a period during which non-

zero occupancy of parasite-occupied patch was observed). Each parameter combination was replicated 25 times. The initial mean host density λ_0 was set to be five fish/patch for all cases. All simulations were conducted in the C++ environment using the R package "*Rcpp*" [43].

Results

Mark-recapture study

Among 215 marked fish hosts (fork length: 62–121 mm), 116 individuals (infected fish, 54 individuals; uninfected fish, 62 individuals) were successfully recaptured and identified (no complete tag loss was observed). The average capture probability of our three-pass electrofishing φ during the recapture session was reasonably high (median: 0.93, 95% CI: 0.83–0.98).

Using the dispersal data as well as the capture history of the marked fish, we developed a Bayesian dispersal model coupled with observation processes (capture probability φ, survival probability *s*, and sampling designs). Estimated survival probability s_{global} during the mark-recapture period was 0.87 (95%CI: 0.62–0.99) with among-individuals variation (σ_s^2) of 6.03 (95%CI: 0.84–17.18). The model also revealed

346 that parasite infection interacted with host body size to modify host dispersal kernels
347 (Table 1). Glochidial infection influenced large fish to be more dispersive, but had
348 opposite effects on small individuals (Fig. 2b). The probability of leaving behind the
349 home subsection was high for large fish hosts (0.76; 80th percentile of body size);
350 specifically, it was 4.3 times greater than that of small fish hosts (0.18; 20th percentile of
351 body size). However, such clear size-dependence in dispersal was not observed for
352 uninfected fish hosts (Fig. 2a). The interactive effect of host body size and parasite
353 infection remained significant even after removing two "super dispersers" (i.e., outliers;
354 only two individuals dispersed ≥ 180 m; see Table S1 and Fig. S1). For raw data, see
355 Fig.S1 in Electronic Supplementary Material.
356 Growth analysis revealed that dispersal costs were size-specific. The main
357 effect of body size and the interaction term with dispersal distance were detected with a
358 probability of ≥ 0.95 (Table 2). The growth of small fish hosts decreased with increasing
359 dispersal distance (Fig. 3). In contrast, this pattern was less apparent for large fish hosts
360 (Fig. 3). The lack of small "super" dispersers likely reflects the size-specific costs of
361 dispersal. Glochidial infection had little effect on fish growth.
362
363 *Simulation*

364 Dispersal plasticity had a strong positive impact on the landscape-level persistence and
365 expansion of the parasite, especially when the host population size was large (see Fig.
366 4b and d; larger values of *y*-axis represent stronger size-dependence in dispersal). The
367 observed plasticity in dispersal led to approximately four times longer persistence of
368 spatially structured parasite population with greater occupancy (~8,000 time steps with
369 ~30% occupancy; filled dot in Fig.4b and d) compared with the weak plastic dispersal
370 scenario (~2,000 time steps with ~6% occupancy; open dot in Fig.4b and d). However,
371 this contrast was not so clear when the host population size was small (Fig. 4a and c).
372
373
374 **Discussion**
375 Host dispersal is now recognized as a key mediator of the landscape-level persistence
376 and expansion of parasites [4-6]. However, the plastic nature of host dispersal responses
377 to parasites has long been underappreciated, despite the fact that intrapopulation
378 variation in phenotype (e.g., body size) is ubiquitous. Inherent difficulties exist in
379 manipulating infection status and quantifying dispersal in natural settings, and these
380 problems have hindered the progress of this research field. Here, using a tractable host-
381 parasite system embedded in a one-dimensional landscape (i.e., a stream), our field

382 experiment overcame these difficulties and provided the first quantitative evidence that
383 parasite infection induces size-dependent host dispersal. Strikingly, our simulation
384 suggested that the observed individual-level variation in host dispersal may greatly
385 enhance parasite persistence and occupancy in a spatially structured system. This is an
386 emergent phenomenon that cannot be understood without the inclusion of among-
387 individuals differences in dispersal propensities. These findings provide an important
388 insight into how parasites emerge, spatially spread, and persist in stochastic natural
389 environments.

390 As *M. laevis* glochidia parasitism occurs mainly in the vicinity of adult mussel
391 aggregations (infection rate drops approximately 0.20 with every hundred meters of
392 distance from aggregation) [15], dispersal seems to be an effective measure to avoid
393 further infection for the salmonid host. Concordant with our hypothesis, there was
394 substantial variation in host dispersal: large fish hosts became more dispersive, whereas
395 small individuals tended to stay in the home patch. This size-specific dispersal is
396 interpretable from the viewpoint of host fitness. In brief, host dispersers cannot benefit
397 from parasite-avoidance unless they survive the dispersal process and reach a new,
398 parasite-free habitat. Our results are consistent with this intuitive prediction. Even under
399 the influence of parasite virulence, the plentiful energy reserves of large salmonid fish

400 may enable them to survive the risky transition process. In contrast, for small fish hosts,
401 glochidia-induced changes (e.g., respiratory burden) [44] may lead to a failure to
402 transition, given their presumed susceptibility to energetic and/or risk costs during
403 dispersal (see [19] for body size effects on swimming performance). Further costs can
404 be levied at the settlement stage, as small salmonid fish are competitively inferior in the
405 dominance hierarchy [17, 18]. Indeed, our growth analysis produced some support for
406 this interpretation, as only small fish hosts incurred dispersal costs (reduced growth; see
407 Fig. 2). Therefore, the net benefits of dispersal are expected to be higher for large fish
408 hosts, but marginal for small fish.

409 Alternatively, it is possible that *M. laevis* glochidia actively manipulated host
410 dispersal behavior. However, *M. laevis* does not seem to have strong incentive for
411 manipulating host dispersal, as the parasite possesses neither a complex life cycle (i.e.,
412 no secondary host) nor specific spawning habitats, both of which are often associated
413 with active host manipulation [7]. Considering the evidence, we suggest that the
414 observed dispersal changes may be a plastic response of salmonid fish hosts, and a
415 “fixed dispersal response” to parasites (e.g., all individuals disperse more; increase in *x*-
416 axis values in Fig. 3) may not be the best option for the host species owing to the size-
417 specific costs of dispersal.

418 Intriguingly, our simulation revealed that the host's plastic response to parasite
419 infection has the potential to increase landscape-level parasite persistence and
420 occupancy, provided that host carrying capacity *K* is high. The rationale behind this
421 finding is the following: large host population sizes ensure a certain fraction of a host
422 population consists of movers (large fish hosts) that allow parasites to colonize distant
423 patches and spread spatially. Meanwhile, stayers (small fish hosts) effectively reinforce
424 (or recolonize) adjacent patches (i.e., the mixture of individual dispersal kernels makes
425 up a "fat-tailed dispersal kernel"). This result deserves further attention. If the observed
426 host response is truly adaptive, then a host's adaptive behavior, either avoiding infection
427 risks or dispersal costs, may lead to undesired consequences: the parasite invades a
428 larger fraction of the patches and persists in the spatially structured system. However,
429 we do not have the valid evidence that dispersal plasticity maintains host fitness (i.e.,
430 adaptive), and further experimentation is needed to confirm this possibility. Future
431 investigations addressing this issue would shed light on how host-parasite interactions
432 are stably sustained in spatially structured systems.
433 Mark-recapture studies are recurrently criticized for the limited coverage of
434 potential dispersal ranges [e.g., 45]. However, our statistical approach is robust against
435 this problem, as we incorporated sampling designs into the dispersal parameter

436 inference (see Eq. 3; individuals that had left the study section were taken into account).
437 This has been shown to provide reliable dispersal parameters, especially when the
438 length of the study stretch is > 4 times greater than the average dispersal distance [46].
439 This likely holds true in our study, as the length of the whole study section (1,200 m)
440 was ~92 times longer than the average dispersal distance of masu salmon (exp(2.57) =
441 13.1 m; see Table 1). Therefore, we are confident in our dispersal parameter inference.
442 Another potential issue would be whether our findings are applicable to
443 horizontally transmissible systems (direct host-to-host transmission). Although our
444 system has several comparative advantages owing to the lack of horizontal transmission
445 (e.g., infection status is readily controllable throughout the experiment), there are
446 certain differences in local transmission dynamics. Nevertheless, we expect that our
447 findings may be equally important in those systems because the landscape-level
448 expansion of horizontally transmissible parasites should also occur mainly through host
449 dispersal. The integration of local horizontal transmission is beyond the scope of our
450 study, but this issue may be a fruitful avenue for future theoretical research.
451 Although the importance of host dispersal has been increasingly appreciated in
452 the field of infectious parasite research, researchers have failed to fully account for the
453 heterogeneous nature of wild organisms. By combining empirical and simulated

approaches, the present study provides a novel parameter (i.e., individual-level variation in host phenotype) for predicting the long-term persistence of parasites and the landscape-level expansion of parasite-contaminated habitats. As intrapopulation heterogeneity of phenotype can be found in almost all animals, our findings may be widely applicable to other host-parasite systems. Future generalization across systems should provide a novel and critical perspective on parasite/disease management issues.

Acknowledgements We thank a member of forest ecosystem management laboratory for their help in the field. We are also grateful to Drs. H. Katahira, N. Ishiyama, Y. Morii and S. Yamanaka for their constructive comments on the early draft of this manuscript.

Author contributions AT and KO designed and conducted the experiment. AT performed statistical analysis and simulation. All authors participated in conception, discussion of the results and manuscript preparation.

Data accessibility

Data and scripts (JAGS and Rcpp) are available at Dryad [47]

(http://dx.doi.org/10.5061/dryad.14mt6).

References

1. Altizer S., Bartel R., Han B.A. 2011 Animal migration and infectious disease risk. *Science* **331**, 296-302.
2. Harvell D., Aronson R., Baron N., Connell J., Dobson A., Ellner S., Gerber L., Kim K., Kuris A., McCallum H. 2004 The rising tide of ocean diseases: unsolved problems and research priorities. *Frontiers in Ecology and the Environment* **2**, 375-382.
3. McCallum H., Barlow N., Hone J. 2001 How should pathogen transmission be modelled? *Trends in Ecology & Evolution* **16**, 295-300.
4. Cross P.C., Lloyd-Smith J.O., Johnson P.L.F., Getz W.M. 2005 Duelling timescales of host movement and disease recovery determine invasion of disease in structured populations. *Ecology Letters* **8**, 587-595.
5. Hess G. 1996 Disease in metapopulation models: implications for conservation. *Ecology* **77**, 1617-1632.
6. Lopez J., Gallinot L., Wade M. 2005 Spread of parasites in metapopulations: an experimental study of the effects of host migration rate and local host population size. *Parasitology* **130**, 323-332.
7. Poulin R. 2007 *Evolutionary ecology of parasites*. Oxfordshire, UK, Princeton University Press.
8. Suhonen J., Honkavaara J., Rantala M.J. 2010 Activation of the immune system promotes insect dispersal in the wild. *Oecologia* **162**, 541-547.
9. Brown G.P., Kelehear C., Pizzatto L., Shine R. 2016 The impact of lungworm parasites on rates of dispersal of their anuran host, the invasive cane toad. *Biological Invasions* **18**, 103-114.
10. Iritani R., Iwasa Y. 2014 Parasite infection drives the evolution of state-dependent dispersal of the host. *Theoretical Population Biology* **92**, 1-13.
11. Smith J.M., Price G.R. 1973 The logic of animal conflict. *Nature* **246**, 15-18.
12. Bonte D., Van Dyck H., Bullock J.M., Coulon A., Delgado M., Gibbs M., Lehouck V., Matthysen E., Mustin K., Saastamoinen M. 2012 Costs of dispersal. *Biological Reviews* **87**, 290-312.
13. Bowler D.E., Benton T.G. 2005 Causes and consequences of animal dispersal strategies: relating individual behaviour to spatial dynamics. *Biological Reviews* **80**, 205-225.
14. Kondo T. 2008 *Monograph of Unionoida in Japan (Mollusca: Bivalvia)*. Tokyo, Malacological Society of Japan.
15. Terui A., Miyazaki Y. 2015 A "parasite-tag" approach reveals long-distance dispersal of the riverine mussel *Margaritifera laevis* by its host fish. *Hydrobiologia* **760**, 189-196.
16. Terui A., Miyazaki Y., Yoshioka A., Kadoya T., Jopp F., Washitani I. 2014 Dispersal of larvae of *Margaritifera laevis* by its host fish. *Freshwater Science* **33**, 112-123.
17. Nakano S. 1995 Individual-differences in resource use, growth and emigration under the

509 influence of a dominance hierarchy in fluvial red-spotted masu salmon in a natural habitat. *Journal of*
510 *Animal Ecology* **64**, 75-84.
511 18. Sato T., Watanabe K. 2014 Do stage-specific functional responses of consumers dampen the
512 effects of subsidies on trophic cascades in streams? *Journal of Animal Ecology* **83**, 907-915.
513 19. Ojanguren A.F., Braña F. 2003 Effects of size and morphology on swimming performance in
514 juvenile brown trout (*Salmo trutta* L.). *Ecology of freshwater fish* **12**, 241-246.
515 20. Haag W.R. 2012 *North American Freshwater Mussels: Natural History, Ecology, and*
516 *Conservation*. New York, USA, Cambridge University Press.
517 21. Lowe W.H. 2009 What drives long-distance dispersal? A test of theoretical predictions.
518 *Ecology* **90**, 1456-1462.
519 22. Awakura T. 1969 On the correlation between the age composition of the freshwater pearl
520 mussel, *Margaritifera laevis* (Haas) and the population size of salmonid fishes. *Scientific Report of the*
521 *Hokkaido Salmon Hatchery* **24**, 55–88.
522 23. Awakura T. 1968 The ecology of parasitic glochidia of the fresh-water pearl mussel,
523 *Margaritifera laevis* (Haas). *Scientific Report of the Hokkaido Salmon Hatchery* **23**, 1-17.
524 24. Hastie L.C., Young M.R. 2001 Freshwater pearl mussel (*Margaritifera margaritifera*)
525 glochidiosis in wild and farmed salmonid stocks in Scotland. *Hydrobiologia* **445**, 109-119.
526 25. Kawai H., Ishiyama N., Hasegawa K., Nakamura F. 2013 The relationship between the
527 snowmelt flood and the establishment of non-native brown trout (*Salmo trutta*) in streams of the Chitose
528 River, Hokkaido, northern Japan. *Ecology of freshwater fish* **22**, 645-653.
529 26. Kobayashi O., Kondo T. 2005 Difference in host preference between two populations of the
530 freshwater pearl mussel *Margaritifera laevis* (Bivalvia: Margaritiferidae) in the Shinano River system,
531 Japan. *Venus* **64**, 63-70.
532 27. Dorazio R.M., Jelks H.L., Jordan F. 2005 Improving removal‐based estimates of abundance
533 by sampling a population of spatially distinct subpopulations. *Biometrics* **61**, 1093-1101.
534 28. Akiyama Y. 2007 Factors causing extinction of a freshwater pearl mussel, *Margaritifera laevis*
535 in Japan (Bivalvia: Unionoida) [thesis]. Sapporo, Hokkaido University.
536 29. Akiyama Y., Iwakuma T. 2007 Survival of glochidial larvae of the freshwater pearl mussel,
537 *Margaritifera laevis* (Bivalvia : Unionoida), at different temperatures: A comparison between two
538 populations with and without recruitment. *Zoological Science* **24**, 890-893.
539 30. Rodriguez M.A. 2002 Restricted movement in stream fish: The paradigm is incomplete, not
540 lost. *Ecology* **83**, 1-13.
541 31. Pepino M., Rodriguez M.A., Magnan P. 2012 Fish dispersal in fragmented landscapes: a
542 modeling framework for quantifying the permeability of structural barriers. *Ecological Applications* **22**,
543 1435-1445.
544 32. Nathan R., Klein E., Robledo-Arnuncio J.J., Revilla E. 2012 Dispersal kernels: review. In

Dispersal Ecology and Evolution (eds. Clobert J., Baguette M., Benton T.G., Bullock J.M.), pp. 187-210. Oxford, UK, Oxford University Press.

33. Denwood M. 2013 runjags: An R package providing interface utilities, parallel computing methods and additional distributions for MCMC models in JAGS. *Journal of Statistical Software* **1**, 0-7.

34. R Core Team (2016). R: A language and environment for statistical computing. R Foundation for Statistical Computing, Vienna, Austria. https://www.R-project.org/. Available at: https://www.R-project.org/ Last accessed 13 July 2016.

35. Gelman A., Hill J. 2007 *Data Analysis Using Regression and Multilevel/Hierarchical Models*. New York, USA, Cambridge University Press.

36. Jackson D., Somers K. 1991 The spectre of 'spurious' correlations. *Oecologia* **86**, 147-151.

37. Grant E.H.C., Nichols J.D., Lowe W.H., Fagan W.F. 2010 Use of multiple dispersal pathways facilitates amphibian persistence in stream networks. *Proceedings of the National Academy of Sciences of the United States of America* **107**, 6936-6940.

38. Krkošek M., Ford J.S., Morton A., Lele S., Myers R.A., Lewis M.A. 2007 Declining wild salmon populations in relation to parasites from farm salmon. *Science* **318**, 1772-1775.

39. Myers R.A., Bowen K.G., Barrowman N.J. 1999 Maximum reproductive rate of fish at low population sizes. *Canadian Journal of Fisheries and Aquatic Sciences* **56**, 2404-2419.

40. Ricker W.E. 1954 Stock and recruitment. *Journal of the Fisheries Board of Canada* **11**, 559-623.

41. Schmidt C., Vandre R. 2010 Ten years of experience in the rearing of young freshwater pearl mussels (*Margaritifera margaritifera*). *Aquatic Conservation-Marine and Freshwater Ecosystems* **20**, 735-747.

42. Hastie L.C., Boon P.J., Young M.R., Way S. 2001 The effects of a major flood on an endangered freshwater mussel population. *Biological Conservation* **98**, 107-115.

43. Eddelbuettel D., François R., Allaire J., Chambers J., Bates D., Ushey K. 2011 Rcpp: Seamless R and C++ integration. *Journal of Statistical Software* **40**, 1-18.

44. Thomas G.R., Taylor J., de Leaniz C.G. 2014 Does the parasitic freshwater pearl mussel *M. margaritifera* harm its host? *Hydrobiologia* **735**, 191-201.

45. Gowan C., Fausch K.D. 1996 Mobile brook trout in two high-elevation Colorado streams: re-evaluating the concept of restricted movement. *Canadian Journal of Fisheries and Aquatic Sciences* **53**, 1370-1381.

46. Pépino M., Rodríguez M.A., Magnan P. 2016 Assessing the detectability of road crossing effects in streams: mark–recapture sampling designs under complex fish movement behaviours. *Journal of Applied Ecology* **53**, 1831-1841.

47. Terui A., Ooue K., Urabe H., Nakamura F. 2017 Data from: Parasite infection induces size-dependent host dispersal: consequences for parasite persistence. Dryad.

581 http://dx.doi.org/10.5061/dryad.14mt6.

582

583

584 **Table 1** Results of the Bayesian model that explains individual-level variation in
585 dispersal kernel. Posterior probability represents the proportion of parameter estimates
586 (MCMC samples) assigned to be either negative or positive. Parameters with a posterior
587 probability of > 0.95 are shown in bold. SE: standard error.

Effect	Estimate	SE	Posterior probability	
			Negative	Positive
Intercept (β_0)	2.571	0.092	-	-
Infection (β_1)	0.151	0.135	0.12	0.88
Body size (β_2)	**0.319**	0.089	0.00	**1.00**
Infection · Size (β_3)	**0.829**	0.185	0.00	**1.00**

588

589 **Table 2** Results of the Bayesian regression model that explains host growth rate.

590 Posterior probability represents the proportion of parameter estimates (MCMC samples)

591 assigned to be either negative or positive. Parameters with a posterior probability of >

592 0.95 are shown in bold. SE: standard error.

Effect	Estimate	SE	Posterior probability	
			Negative	Positive
Intercept	0.098	0.006	-	-
Body size	**−0.016**	0.006	**1.00**	0.00
Dispersal distance	−0.009	0.010	0.82	0.18
Infection	0.003	0.009	0.36	0.64
Size · Distance	**0.013**	0.007	0.05	**0.95**
Size · Infection	0.008	0.009	0.19	0.81
Infection · Distance	−0.008	0.010	0.81	0.19

593

Figure captions

Fig. 1 Schematic representation of the life cycle of the freshwater mussel *Margaritifera laevis*. Glochidia released from female mussels infect the gills of masu salmon *Oncorhynchus masou masou* in the local habitat (local infection process). After a 40–50-day parasitic period, juvenile mussels detach from host fish and invade into unoccupied, parasite-free habitats through host dispersal (landscape-level process).

Fig. 2 Plastic dispersal response of masu salmon *Oncorhynchus masou masou* to infection by larval parasites of *Margaritifera laevis*. Shaded areas with dotted lines denote average dispersal kernels. Solid and dashed lines indicate dispersal kernels for large (80^{th} percentile body size) and small (20^{th} percentile body size) fish hosts, respectively. Uninfected individuals showed little variation in dispersal (a). In contrast, infected individuals exhibited strong size-dependence in dispersal (b).

Fig. 3 Size-specific effects of dispersal on host growth rates ($\log(FL_{50}/FL_0)$). Solid and broken lines represent predicted values of the linear mixed effect model for large (80^{th} percentile body size) and small (20^{th} percentile body size) fish hosts, respectively. Bubbles indicate individual fish and their sizes are proportional to fork length during the

612 first capture session (FL_0).

613

614 **Fig. 4** Contour plots of simulated parasite persistence times (a, b) and occupancy
615 (proportion of parasite-occupied patch; c, d) in a 100-patch linear landscape with host
616 carrying capacities of 4 (a, c) and 8 fish/patch (b, d). Brighter colors represent longer
617 persistence time (a, b) or greater occupancy (c, d). Increasing values on the γ (x-axis)
618 denote increasing average dispersal distance, whereas increasing values on the δ (y-axis)
619 represent stronger size-dependence in dispersal (larger individuals become more
620 dispersive whereas smaller individuals become less dispersive). Other parameter values
621 were as follows: colonization rate, $C = 0.005$; extinction probability, $E = 0.01$;
622 environmental stochasticity in host population dynamics, $\sigma_\varepsilon = 0.18$; and survival during
623 dispersal, $s = 0.87$. Open and filled dots represent observed dispersal scenarios with
624 weak ($\gamma = \beta_0$, $\delta = \beta_2$; see Fig. 1a) and strong ($\gamma = \beta_0 + \beta_1$, $\delta = \beta_2 + \beta_3$; see Fig. 1b) size-
625 dependence, respectively. See Table 1 for estimated parameters.

626

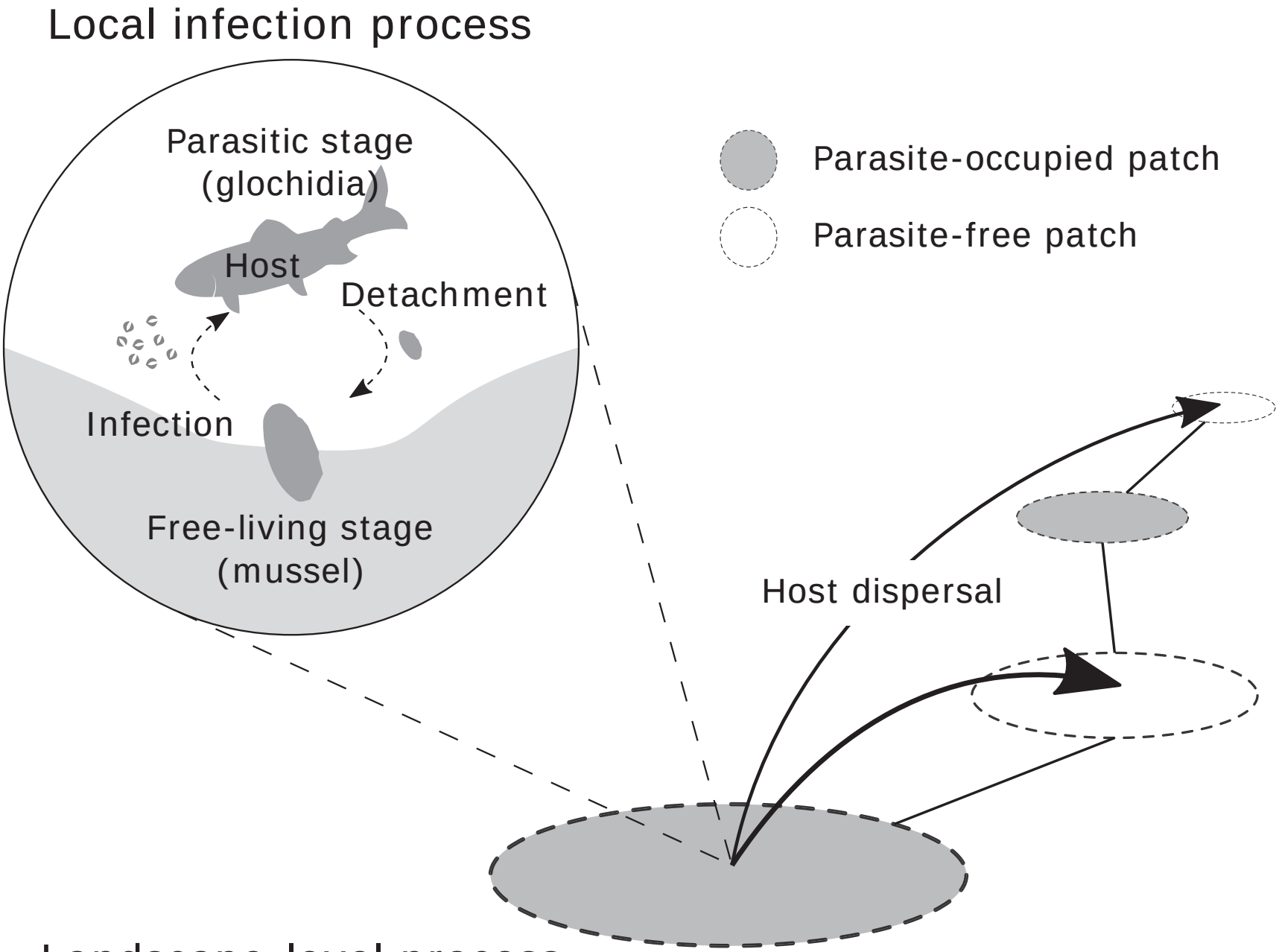

Fig. 1 Terui et al.

Fig. 2 Terui et al.

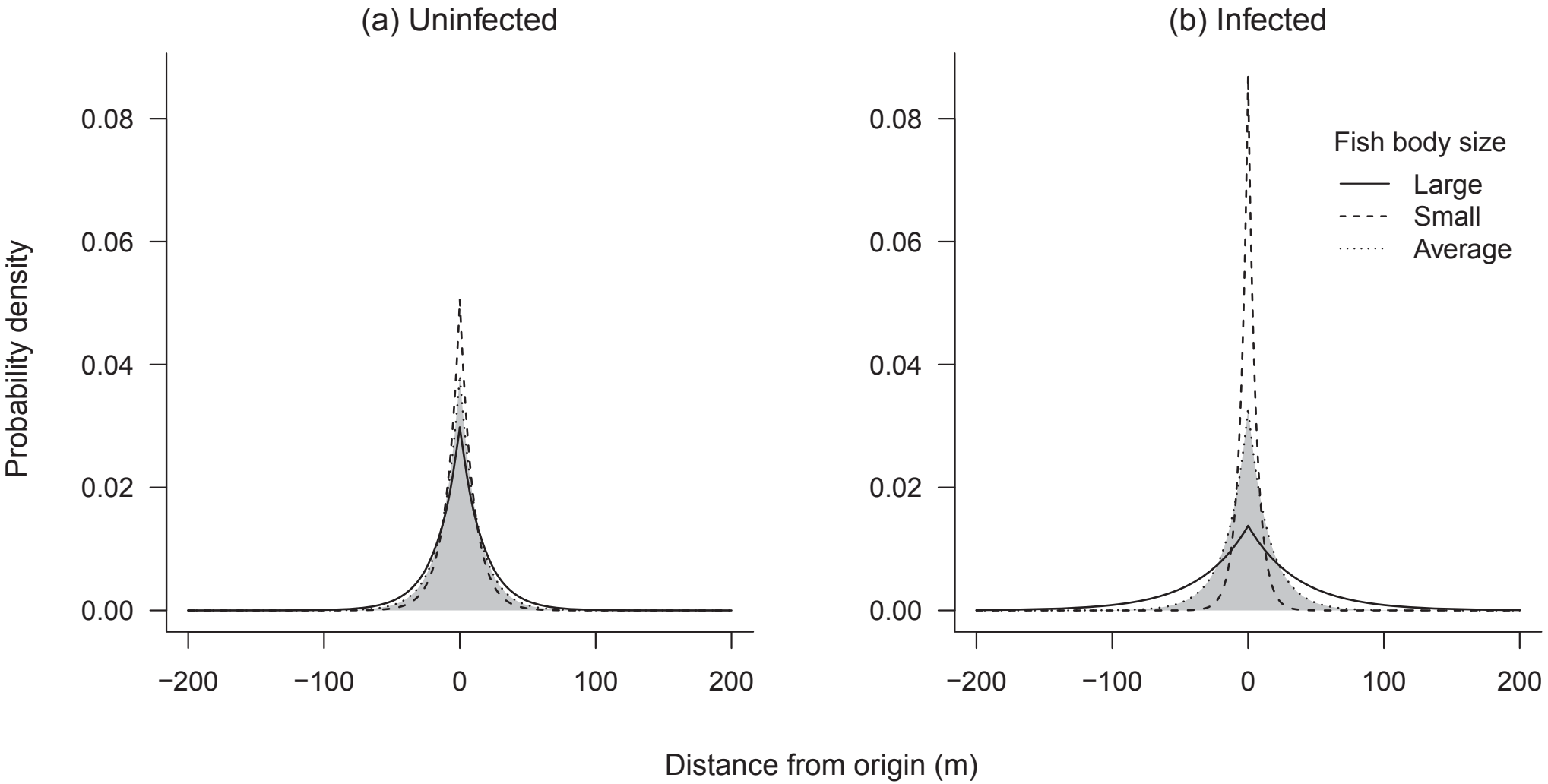

Fig. 3 Terui et al.

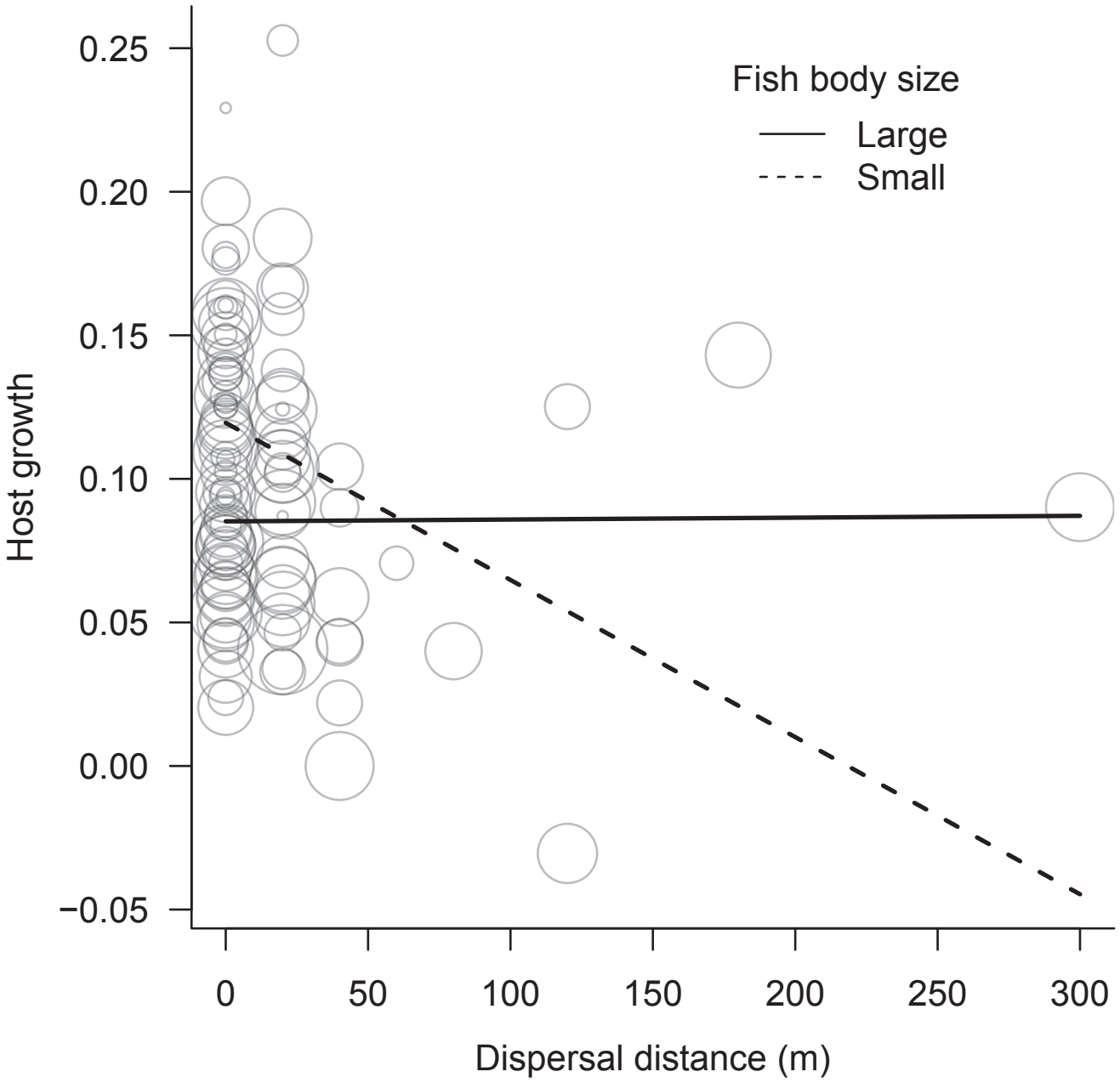

Fig.4 Terui et al.